Master's Thesis

A viscoelastic efficient higher-order plate theory for composite laminates

February 2014

Graduate School of Seoul National University

Department of Mechanical & Aerospace Engineering

Nguyen Sy Ngoc

Abstract

A viscoelastic efficient higher-order plate theory for composite laminates

Ngoc, Nguyen Sy
School of Mechanical and Aerospace Engineering
The Graduate School
Seoul National University

An efficient higher-order plate theory for viscoelastic materials is developed to obtain the accurate and efficient time-dependent mechanical behaviors of composite laminates. In-plane displacement fields are constructed by superimposing a cubic varying displacement field on a linear zigzag varying field. Time-dependent relaxation modulus has the form of Prony series which can be determined by the master curve based on experimental data. The constitutive equation which has the form of Boltzmann superposition integral for linear viscoelastic materials is simplified by convolution theorem in the Laplace transformed domain to avoid direct integration as well as to improve both computational accuracy and efficiency. Moreover, by using linear elastic stress-strain relationship in the corresponding Laplace domain, the transverse shear stress free conditions at the top and bottom surfaces and the transverse shear stress continuity conditions at the interface between layers can be satisfied conveniently to reduce the number of primary unknown variables. To validate

the present theory, the viscoelastic responses in the real time domain are obtained through various numerical inverse Laplace transforms. The numerical results for graphite/epoxy GY70/339 material are obtained and compared with the solutions of elastic composite laminated plates.

Keywords: Viscoelastic, Composite laminate, Efficient Higher-Order Plate Theory, Laplace transform.

Student Number: 2011-24057

Contents

Nomenclasture

h	=	total thickness of the laminate
J_{ijkl}	=	compliances modulus
Q_{ijkl}	=	relaxation modulus
u_α, w	=	displacement along the x_α or z axis
σ_{ij}	=	stress tensor components
ε_{kl}	=	strain tensor components
t	=	time
t'	=	dummy variable of time for integration
φ_{ijkl}	=	time-dependent function of relaxation modulus
b_{ijkl}	=	viscoelastic coefficient in the generalized coordinates
τ_{ijkl}	=	viscoelastic characteristic time
s	=	variable in Laplace domain
n	=	number of layers of the laminates
θ_k	=	the angle of k-th layer
u_α^0, χ_α, ξ_α, ϕ_α, S_α^k, w	=	primary unknown variables in time domain
$H(z\text{-}z_k)$	=	Heaviside unit step function

$u_\alpha^{*0}, u_\alpha^{*1}, u_\alpha^{*2}, u_\alpha^{*3}, u_\alpha^{*k}, w^*$	=	primary unknown variables in Laplace domain
$N_{\alpha\beta}, M_{\alpha\beta}, R_{\alpha\beta}^2, R_{\alpha\beta}^3, Q_\alpha, V_\alpha^1, V_\alpha^2, N_{\alpha\beta}^k, M_{\alpha\beta}^k, Q_\alpha^k$	=	resultants of internal forces and moments in time domain
$\bar{N}_{\alpha\beta}, \bar{M}_{\alpha\beta}, \bar{R}_{\alpha\beta}^2, \bar{R}_{\alpha\beta}^3, \bar{Q}_\alpha, \bar{V}_\alpha^1, \bar{V}_\alpha^2, \bar{N}_{\alpha\beta}^k, \bar{M}_{\alpha\beta}^k, \bar{Q}_\alpha^k$	=	resultants of internal forces and moments in Laplace domain
$\breve{N}_\alpha, \breve{M}_\alpha, \breve{R}_\alpha^2, \breve{R}_\alpha^3, \breve{N}_0^f, \breve{W}$	=	resultants of inertia forces in Laplace domain
$u_\alpha^{**0}, u_\alpha^{**1}, u_\alpha^{**2}, u_\alpha^{**3}, u_\alpha^{**k}, w^{**}$	=	acceleration variables in Laplace domain
I_c, I_c^k	=	integrations of density through the thickness
$A_{ijkl}^q, A_{ijkl}^{qk}$	=	components of laminate stiffness matrix
$p, \bar{p}$	=	function of transverse distributed force intensity in time and Laplace domains
L	=	side length of plate
K	=	stiffness matrix
M	=	mass matrix
S	=	the length-to-height ratio
ρ	=	mass density

List of Figures

List of Tables

Chapter 1. Introduction

Recently, multilayered composite structures have been increasingly used in various engineering fields such as automotive, marine, and aerospace industry which require high stiffness and strength to weight ratio. Due to these advantages, laminated composites have been applied and expanded their application continuously to high engineering structural areas for last three decades.

These applications require accurate prediction of the mechanical and thermo-mechanical behaviors of composite laminates for the analysis and design of structural composites. Thus, a lot of computational models [1-5] have been developed to overcome lack of accuracy of the classical laminated plate theory (CLPT) which underestimates the deflections and overestimates natural frequencies and buckling loads. These inaccuracies are the consequence of neglecting the effects of transverse shear deformation (TSD). To improve this situation, various refined theories considering the effects of TSD have been developed. For example, first-order shear deformation theory (FSDT) considers TSD of the plate requiring the shear correction factor [5, 6]. Even though the FSDT is more reliable than CLPT, it still cannot predict the detailed through the thickness mechanical behaviors accurately. Hence, third-order shear deformation theory (TSDT) using a cubic polynomial for the in-plane displacement fields is proposed to improve accuracy as well as avoid using

shear correction factors [7]. Nevertheless, TSDT is only adequate in the prediction of global responses such as deflection, natural frequency and buckling load. It fails to describe the local responses such as in-plane displacement and stress distributions of laminates in each layer. In order to predict both global and local behavior in thick multilayered plates accurately, Cho and Parmerter [8-11] have developed efficient higher-order plate theory (EHOPT) by combining a linear zigzag and a cubic varying in-plane displacement field. Moreover, the number of unknown variables of EHOPT is the same as that of FSDT and does not depend upon the number of layers. Thus, EHOPT is very efficient for analyzing laminated composite plates with a large number of layers and gives reliable results compared to the exact elasticity solution. With these advantages, EHOPT has been extended to various applications: post process method, strain energy transformation, thermo-electro-mechanical problem, multiple-delamination and vibration analysis [12-17].

However, in all these studies using EHOPT, the materials considered in the analysis have been limited to linear elastic ones with the assumption that the relaxation modulus is independent of time. Actually, the laminated composite consists of elastic fibers and viscoelastic matrix. Therefore, in high temperature environment, the mechanical behaviors of laminated composites lead to creep and relaxation responses because of the time-dependent properties of viscoelastic matrix [18]. For instance, Crossman has determined relaxation modulus as the function of time in the form of Prony series for graphite/epoxy T300/934, T300/5209, and GY70/339 composite materials [19].

On the other hand, to study the time-dependent behavior of laminated composites, several researches have analyzed the dynamic response of the composite laminates considering the viscoelastic effect. However, the previous works have some limitations:

Firstly, the Boltzmann superposition principle as the constitutive equation for viscoelastic materials in integral form has been utilized to be solved by numerical procedures based on Taylor method [20-23] or trapezoidal method [24]. The computational accuracy depends on a time step Δt. To achieve the solution at the time t, it needs enormous computational resources for many repetitive solutions for each time step. Especially, such error significantly increases for long-term problems. Thus, this approach is not effective in the analysis of viscoelastic behaviors because of extensive computational storage requirements.

To avoid the above-mentioned limitation, some researchers [25-28] have introduced the Laplace or Fourier transforms. The results in real time domain are obtained by inverse Laplace transforms based on numerical calculations. Therefore, these methods seem to be effective for long-term problems of viscoelastic analysis. However, the accuracy of previous works is limited for multilayered plate because of employing FSDT or TSDT.

Lastly, many researches [23, 25-28] have assumed viscoelastic behavior as simple of analog models constructed from linear springs and dashpots such as Maxwell model, Kelvin model or simple Prony series with low number of terms. However, relaxation modulus of real composite materials is much more complicated. Indeed, the properties of some real composite materials such as

GY70/339, T300/5209 and T300/934 have been experimentally characterized [19]. It is necessary to express the time-dependent relaxation moduli of these composites as many-term Prony series obtained by mastering curves experimental data.

In the present study, the mechanical behaviors of viscoelastic composite laminates are investigated by applying Laplace transforms based on the accurate and efficient method (EHOPT) for the real composite material GY70/339 at the room temperature and moisture ($T=75^{o}F$, $M=0.1\%$). By applying Laplace transformation instead of direct time integrations of Boltzmann superposition equation and inversing in the time domain, the computational accuracy increases significantly [29-33]. Because of EHOPT's advantages, both global and local time-dependent mechanical behaviors such as deflections, in-plane displacement, in-plane normal stress and transverse shear stress can be analyzed adequately. In addition, by employing Laplace transform, the top and bottom transverse shear stress free conditions as well as continuity conditions at interface layers are conveniently applied, which makes the degrees of freedom of the proposed method be much smaller than those of the layerwise one. The properties of real material graphite/epoxy GY70/339 with the time-dependent relaxation modulus in many-term Prony series form are employed. Numerical results are demonstrated to prove accuracy and efficiency of the present model.

Chapter 2. Mathematical Formulation

2.1. Governing Equations for Linear Viscoelastic Material

As the constitutive equation of viscoelastic materials, the Boltzmann's superposition principle for linear viscoelastic materials is employed as follows:

$$\sigma_{ij}(t) = \int_0^t Q^0_{ijkl}(t-t') \frac{\partial \varepsilon_{kl}(t')}{\partial t'} dt'$$
$$\varepsilon_{ij}(t) = \int_0^t J^0_{ijkl}(t-t') \frac{\partial \sigma_{kl}(t')}{\partial t'} dt' \quad (1)$$

where t denotes time, t' is a dummy variable for integration, $\sigma_{ij}(t)$ and $\varepsilon_{kl}(t)$ are the time-dependent stress and strain, respectively. $J_{ijkl}{}^0(t)$ is a compliance and $Q_{ijkl}{}^0(t)$ is a relaxation modulus which can be represented by a series of decaying exponentials, as in a Prony series:

$$Q^0_{ijkl}(t) = Q_{ijkl}\varphi_{ijkl}(t) = Q_{ijkl}\left(1 + \sum_{p=1}^{m} b^p_{ijkl} e^{-\frac{t}{\tau^p_{ijkl}}}\right) \quad (2)$$

where the initial relaxation modulus Q_{ijkl} can be determined by the elastic properties; the viscoelastic coefficients $b_{ijkl}{}^p$ and the characteristic time $\tau_{ijkl}{}^p$ can be obtained by experimental relaxation curves.

It is assumed that Q_{1111} is independent of time (φ_{1111}=1) since the property in the longitudinal direction shows fiber dominant characteristics. Other moduli have the same time-dependent function (φ_{ijkl}= $\varphi(t)$) with each other because of

matrix dominant characteristic. Therefore, for 3-D orthotropic materials, the constitutive equations for orthotropic layers in the principal axes system of the materials can be expressed as follows:

$$\begin{pmatrix}\sigma_{11}(t)\\ \sigma_{22}(t)\\ \sigma_{12}(t)\end{pmatrix}=\int_0^t\begin{bmatrix} Q_{1111} & Q_{1122}\,\varphi_{ijkl}(t-t') & 0\\ Q_{2211}\,\varphi_{ijkl}(t-t') & Q_{2222}\,\varphi_{ijkl}(t-t') & 0\\ 0 & 0 & Q_{1212}\,\varphi_{ijkl}(t-t')\end{bmatrix}\frac{\partial}{\partial t'}\begin{pmatrix}\varepsilon_{11}(t')\\ \varepsilon_{22}(t')\\ \varepsilon_{12}(t')\end{pmatrix}dt' \quad (3a)$$

$$\begin{pmatrix}\sigma_{32}(t)\\ \sigma_{31}(t)\end{pmatrix}=\int_0^t\begin{bmatrix} Q_{3232}\,\varphi_{ijkl}(t-t') & 0\\ 0 & Q_{3131}\,\varphi_{ijkl}(t-t')\end{bmatrix}\frac{\partial}{\partial t'}\begin{pmatrix}\varepsilon_{32}(t')\\ \varepsilon_{31}(t')\end{pmatrix}dt' \quad (3b)$$

By taking the Laplace transform with respect to the time, the Boltzmann superposition integral equation in Laplace domain can be derived as follows:

$$\begin{pmatrix}\sigma_{11}^*(s)\\ \sigma_{22}^*(s)\\ \sigma_{12}^*(s)\end{pmatrix}=\begin{bmatrix} Q_{1111}\dfrac{1}{s} & Q_{1122}\,\varphi^*(s) & 0\\ Q_{2211}\,\varphi^*(s) & Q_{2222}\,\varphi^*(s) & 0\\ 0 & 0 & Q_{1212}\,\varphi^*(s)\end{bmatrix}s\begin{pmatrix}\varepsilon_{11}^*(s)\\ \varepsilon_{22}^*(s)\\ \varepsilon_{12}^*(s)\end{pmatrix} \quad (4a)$$

$$\begin{pmatrix}\sigma_{32}^*(s)\\ \sigma_{31}^*(s)\end{pmatrix}=\begin{bmatrix} Q_{3232}\,\varphi^*(s) & 0\\ 0 & Q_{3131}\,\varphi^*(s)\end{bmatrix}s\begin{pmatrix}\varepsilon_{32}^*(s)\\ \varepsilon_{31}^*(s)\end{pmatrix} \quad (4b)$$

where ( )* are parameters in the Laplace domain. It is well recognized that the form of Boltzmann superposition integral equation in the Laplace domain for viscoelastic material reduces to linear elastic Hook's law. Hence, it is possible to analyze the viscoelastic laminated composite plates in the Laplace domain as the same elastic counterpart.

2.2. Efficient Higher-Order Plate Theory for Viscoelastic Material

Unidirectional composite laminates with rectangular geometry is shown in Fig. 1a, with the n layers and the thickness h. The mid-plane of laminated plate is considered as reference plane. The fibers of the k^{th} lamina are oriented at an angle θ_k to the x_1-axis. Considering the material anisotropies of the composite laminates, the in-plane displacement fields can be assumed as the one of the original EHOPT [8, 9], which superimposes linear zigzag displacements, with different slope in each layer, on an overall cubic varying field. The plane stress assumption is applied and the transverse displacement field is assumed to be constant along the thickness direction. Therefore, the deflection w is only a function of the in-plane coordinates. The displacement fields are assumed as follows:

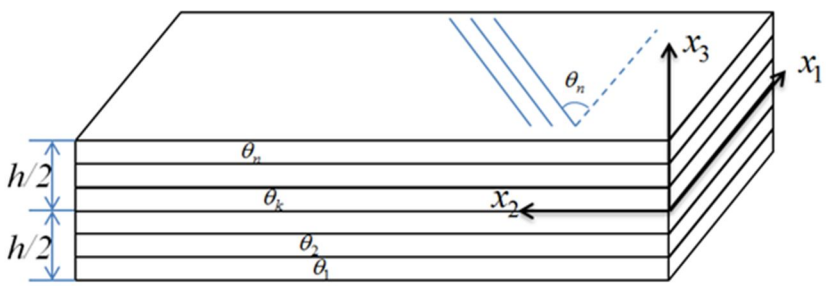

Figure 1a. Geometry and coordinates of rectangular laminated plates

$$u_\alpha(x,y,z,t) = u_\alpha^0(x,y,t) + \chi_\alpha(x,y,t)z + \xi_\alpha(x,y,t)z^2 + \phi_\alpha(x,y,t)z^3 + \sum_{k=1}^{n-1} S_\alpha^k(x,y,t)(z-z_k)H(z-z_k) \quad (6)$$

$$u_3(x,y,t) = w(x,y,t)$$

where $u_\alpha{}^0$ and w are displacements defined at the mid-plane of the laminated plates. n is the number of layers, and $H(z\text{-}z_k)$ is the Heaviside unit step function. A schematic of the layup configuration and in-plane displacement field is shown in Fig. 1b. It is worth to note that all of relaxation moduli and slopes depend on the time for viscoelastic laminates.

Following EHOPT, to reduce number of unknown primary variables in the in-plane displacement fields, the requirements that the transverse stress should

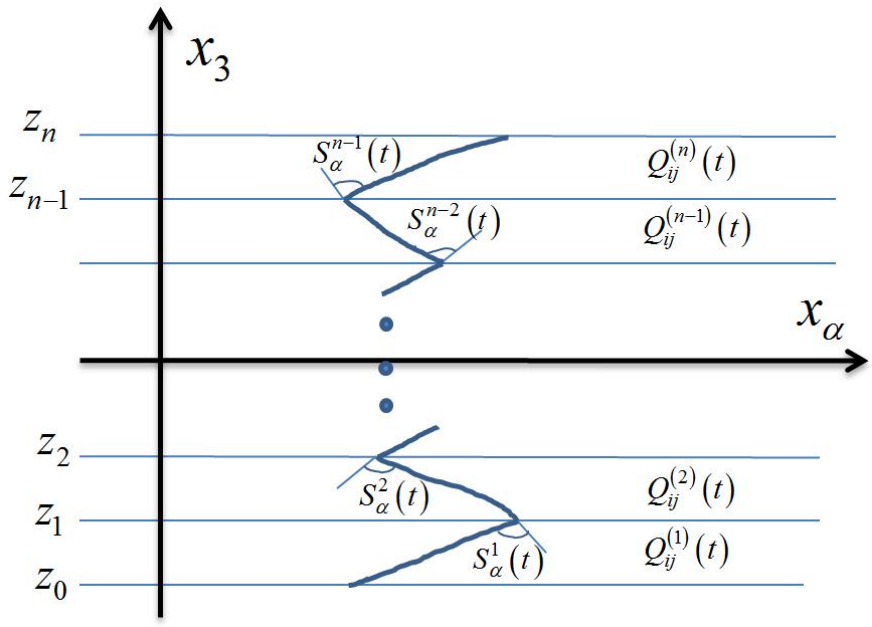

Figure 2b. In-plane displacement field configuration of laminated composite plates.

be vanished on the top and bottom surface of the plate, and be continuous at interface between layers are imposed. There are unknown variables S_α^k in the displacement fields depending on the number of layers. Thus, traction free boundary conditions for the top and bottom surface of the plate $\sigma_{\alpha 3}|_{z=\pm h/2}=0$ are utilized to reduce unknown variables in Laplace domain, as follows:

$$\begin{aligned}\xi_\gamma^*(s) &= -\frac{1}{2h}\sum_{k=1}^{n-1} S_\gamma^{k*}(s) \\ \chi_\gamma^*(s) &= -\left[\frac{3h^2}{4}\phi_\gamma^*(s) + w_{,\gamma}^*(s) + \frac{1}{2}\sum_{k=1}^{n-1} S_\gamma^{k*}(s)\right]\end{aligned} \tag{7}$$

Moreover, the transverse shear stress continuity conditions at the interfaces between the layers should be imposed to reduce the layer-dependent variables S_γ^{k*} in Laplace domain $S_\gamma^{k*}=b_{\alpha\gamma}{}^k\phi_\gamma{}^*$. Hence, the displacement fields in Laplace domain are written as follows:

$$\begin{aligned}u_\alpha^* &= u_\alpha^{*0} + u_\alpha^{*1} z + u_\alpha^{*2} z^2 + u_\alpha^{*3} z^3 + \sum_{k=1}^{n-1} u_\alpha^{*k}(z - z_k) H(z - z_k) \\ u^* &= w^*\end{aligned} \tag{8}$$

where

$$\begin{aligned} u_\alpha^{*1} &= c_{\alpha\gamma}\phi_\gamma^* - w_{,\alpha}^* & u_\alpha^{*2} &= -\frac{1}{2h}\sum_{k=1}^{n-1} b_{\alpha\gamma}^k \phi_\gamma^* \\ u_\alpha^{*3} &= \phi_\alpha^* & u_\alpha^{*k} &= b_{\alpha\gamma}^k \phi_\gamma^* \end{aligned} \tag{9}$$

where $b_{\alpha\gamma}{}^k$ and $c_{\alpha\gamma}$ denote the matrices in the Laplace transformed domain which depend on both the material properties and the thickness of each ply. The

procedure determining $b_{\alpha\gamma}{}^{k}$ and $c_{\alpha\gamma}$ is shown in Appendix 1. It is well recognized that all of $u_{\alpha}{}^{*0}$, $\phi_{\gamma}{}^{*}$, $b_{\alpha\gamma}{}^{k}$ and $c_{\alpha\gamma}$ are functions of s in Laplace domain. The number of primary variables in Laplace domain is the same as that of FSDT, and they are independent of the number of layers.

By using the Hamilton's principle and integrating by parts, the following equilibrium equations are obtained as follows:

$$\left(\int_{v}\sigma_{\alpha\beta}\delta\varepsilon_{\alpha\beta}dv+\int_{v}\sigma_{\alpha 3}\delta\gamma_{\alpha 3}dv\right)+\int_{v}\rho\left(\ddot{u}_{\alpha}\delta u_{\alpha}+\ddot{w}\delta w\right)dv-\int_{A}p\delta w dA=0 \tag{10}$$

$$\begin{aligned}
&\delta u_{\alpha}^{*0}:-\bar{N}_{\alpha\beta,\beta}^{0}+\breve{N}_{\alpha}=0\\
&\delta\phi_{\alpha}^{*}:-\left(\bar{M}_{\gamma\beta,\beta}c_{\gamma\alpha}-\frac{1}{2h}\sum_{k=1}^{n-1}b_{\gamma\alpha}^{k}\bar{R}_{\gamma\beta,\beta}^{2}+\bar{R}_{\alpha\beta,\beta}^{3}+\sum_{k=1}^{n-1}b_{\gamma\alpha}^{k}(\bar{M}_{\gamma\beta,\beta}^{k}-z_{k}\bar{N}_{\gamma\beta,\beta}^{k})\right)\\
&\quad+\left(c_{\gamma\alpha}\bar{Q}_{\gamma}-\frac{1}{h}\sum_{k=1}^{n-1}b_{\gamma\alpha}^{k}\bar{V}_{\gamma}^{1}+3\bar{V}_{\alpha}^{2}+\sum_{k=1}^{n-1}b_{\gamma\alpha}^{k}\bar{Q}_{\gamma}^{k}\right)\\
&\quad+\left[c_{\gamma\alpha}\breve{M}_{\gamma}-\frac{1}{2h}\sum_{k=1}^{n-1}b_{\gamma\alpha}^{k}\breve{R}_{\gamma}^{2}+\breve{R}_{\alpha}^{3}+\sum_{f=1}^{n-1}b_{\gamma\alpha}^{f}\left(\breve{M}_{\gamma}^{f}-z_{f}\breve{N}_{\gamma}^{f}\right)\right]=0\\
&\delta w^{*}:-\bar{M}_{\alpha\beta,\alpha\beta}+\breve{M}_{\alpha,\alpha}+\bar{W}-\bar{p}=0
\end{aligned} \tag{11}$$

where the stress resultants are defined as follows:

$$\left\{N_{\alpha\beta},M_{\alpha\beta},R_{\alpha\beta}^{2},R_{\alpha\beta}^{3}\right\}=\int_{-h/2}^{h/2}\sigma_{\alpha\beta}\left\{1,z,z^{2},z^{3}\right\}dz \tag{12a}$$

$$\left\{Q_{\alpha},V_{\alpha}^{1},V_{\alpha}^{2}\right\}=\int_{-h/2}^{h/2}\sigma_{\alpha 3}\left\{1,z,z^{2}\right\}dz \tag{12b}$$

$$\left\{N_{\alpha\beta}^{k},M_{\alpha\beta}^{k}\right\}=\int_{-h/2}^{h/2}\sigma_{\alpha\beta}\left\{1,z\right\}H\left(z-z_{k}\right)dz=\int_{z_{k}}^{h/2}\sigma_{\alpha\beta}\left\{1,z\right\}dz \tag{12c}$$

$$Q_{\alpha}^{k}=\int_{-h/2}^{h/2}\sigma_{\alpha 3}H\left(z-z_{k}\right)dz=\int_{z_{k}}^{h/2}\sigma_{\alpha 3}dz \tag{12d}$$

$$\left(\bar{N}_{\alpha\beta},\bar{M}_{\alpha\beta},\bar{R}^2_{\alpha\beta},\bar{R}^3_{\alpha\beta},\bar{Q}_{\alpha},\bar{V}^1_{\alpha},\bar{V}^2_{\alpha},\bar{N}^k_{\alpha\beta},\bar{M}^k_{\alpha\beta},\bar{Q}^k_{\alpha}\right) = \mathcal{L}\left(N_{\alpha\beta},M_{\alpha\beta},R^2_{\alpha\beta},R^3_{\alpha\beta},Q_{\alpha},V^1_{\alpha},V^2_{\alpha},N^k_{\alpha\beta},M^k_{\alpha\beta},Q^k_{\alpha}\right) \tag{13}$$

$$\breve{N}_{\alpha} = I_0 u^{**0}_{\alpha} + I_1 u^{**1}_{\alpha} + I_2 u^{**2}_{\alpha} + I_3 u^{**3}_{\alpha} + \sum_{k=1}^{n-1} u^{**k}_{\alpha}\left(I^k_1 - z_k I^k_0\right)$$
$$\breve{W} = I_0 w^{**} \tag{14}$$

where

$$\begin{aligned} u^{**0}_{\alpha}(s) &= u^{*0}_{\alpha}s^2 - s\dot{u}^0_{\alpha}(0) - \ddot{u}^0_{\alpha}(0) & u^{**1}_{\alpha}(s) &= u^{*1}_{\alpha}s^2 - s\dot{u}^1_{\alpha}(0) - \ddot{u}^1_{\alpha}(0) \\ u^{**2}_{\alpha}(s) &= u^{*2}_{\alpha}s^2 - s\dot{u}^2_{\alpha}(0) - \ddot{u}^2_{\alpha}(0) & u^{**3}_{\alpha}(s) &= u^{*3}_{\alpha}s^2 - s\dot{u}^3_{\alpha}(0) - \ddot{u}^3_{\alpha}(0) \\ u^{**k}_{\alpha}(s) &= u^{*k}_{\alpha}s^2 - s\dot{u}^k_{\alpha}(0) - \ddot{u}^k_{\alpha}(0) & w^{**}(s) &= w^{*}s^2 - s\dot{w}(0) - \ddot{w}(0) \end{aligned} \tag{15}$$

and

$$I_c = \int_{-h/2}^{h/2} \rho z^c dz \qquad I^k_c = \int_{z_k}^{h/2} \rho z^c dz \tag{16}$$

$\breve{M}_{\alpha}, \breve{R}^2_{\alpha}, \breve{R}^3_{\alpha}, \breve{N}^f_0$ and $\breve{M}^f_{\alpha}$ have the similar forms with $\breve{N}_{\alpha}$. These resultants in Laplace domain can be expressed as follows:

$$\begin{aligned} \bar{N}_{\alpha\beta} = \Big\{ & A^{0*}_{\alpha\beta\gamma\delta}u^{*0}_{\gamma,\delta} + A^{1*}_{\alpha\beta\gamma\delta}\left(c_{\gamma\alpha}\phi^*_{\alpha,\delta} - w^*_{,\gamma\delta}\right) - \frac{1}{2h}A^{2*}_{\alpha\beta\gamma\delta}\sum_{k=1}^{n-1}b^k_{\gamma\alpha}\phi^*_{\alpha,\delta} \\ & + A^{3*}_{\alpha\beta\gamma\delta}\phi^*_{\gamma,\delta} + \sum_{k=1}^{n-1}\left[A^{1k*}_{\alpha\beta\gamma\delta} - z_k A^{0k*}_{\alpha\beta\gamma\delta}\right]b^k_{\gamma\alpha}\phi^*_{\alpha,\delta}\Big\} \end{aligned} \tag{17a}$$

$$\bar{Q}_{\gamma} = \left\{\frac{1}{2}A^{0*}_{\gamma 3\alpha 3}c_{\alpha\gamma}\phi^*_{\gamma} - \frac{1}{2h}A^{1*}_{\gamma 3\alpha 3}\sum_{k=1}^{n-1}b^k_{\alpha\gamma}\phi^*_{\gamma} + \frac{3}{2}A^{2*}_{\gamma 3\alpha 3}\phi^*_{\alpha} + \frac{1}{2}\sum_{k=1}^{n-1}A^{0k*}_{\gamma 3\alpha 3}b^k_{\alpha\gamma}\phi^*_{\gamma}\right\} \tag{17b}$$

where $A_{ijkl}{}^{q*}$ and $A_{ijkl}{}^{qk*}$ are defined as follows:

$$A_{ijkl}^{q*}(s)=\int_{-h/2}^{h/2}Q_{ijkl}^{*}(s)z^{q}dz=\sum_{m=0}^{n-1}\left\{\int_{z_m}^{z_{m+1}}Q_{ijkl}^{m*}(s)z^{q}dz\right\}$$
$$=\frac{1}{q+1}\sum_{m=0}^{n-1}Q_{ijkl}^{m*}(s)\left(z_{m+1}^{q+1}-z_{m}^{q+1}\right) \tag{18a}$$

$$A_{ijkl}^{qk*}(s)=\int_{z_k}^{h/2}Q_{ijkl}^{*}(s)z^{q}dz=\sum_{m=k}^{n-1}\left\{\int_{z_m}^{z_{m+1}}Q_{ijkl}^{m*}(s)z^{q}dz\right\}$$
$$=\frac{1}{q+1}\sum_{m=k}^{n-1}Q_{ijkl}^{m*}(s)\left(z_{m+1}^{q+1}-z_{m}^{q+1}\right) \tag{18b}$$

$\bar{M}_{\alpha\beta},\bar{R}_{\alpha\beta}^{2},\bar{R}_{\alpha\beta}^{3},\bar{N}_{\alpha\beta}^{k}$ and $\bar{M}_{\alpha\beta}^{k}$ have the similar forms with $\bar{N}_{\alpha\beta}$; $\bar{V}_{\alpha}^{1},\bar{V}_{\alpha}^{2}$ and $\bar{Q}_{\alpha}^{k}$ have the similar forms with $\bar{Q}_{\gamma}$.

Chapter 3. Numerical results for cylindrical bending of laminated plates

For the both static and harmonic loadings, the cylindrical bending of laminated plate is analyzed as numerical examples. Thus, all of equilibrium equations are reduced to one-dimensional form. The displacement variables are assumed as trigonometric functions to satisfy the simply supported boundary conditions. In the real time domain, the displacement and transverse load can be chosen to be the following forms:

$$\begin{aligned} u_\gamma^0(x,t) &= \sum_{n=1}^{\infty} U_{\gamma(n)}^0(t)\cos(n\alpha x) \\ \phi_\gamma(x,t) &= \sum_{n=1}^{\infty} \Phi_{\gamma(n)}(t)\cos(n\alpha x) \\ w(x,t) &= \sum_{n=1}^{\infty} W_{(n)}(t)\sin(n\alpha x) \\ p(x,t) &= \sum_{n=1}^{\infty} p_{(n)}(t)\sin(n\alpha x) \end{aligned} \tag{19a}$$

Hence, the displacement and applied load in Laplace domain can be expressed as follows:

$$
\begin{aligned}
u_{\gamma}^{*0}(x,s) &= \sum_{n=1}^{\infty} U_{\gamma(n)}^{*0}(s)\cos(n\alpha x) \\
\phi_{\gamma}^{*}(x,s) &= \sum_{n=1}^{\infty} \Phi_{\gamma(n)}^{*}(s)\cos(n\alpha x) \\
w^{*}(x,s) &= \sum_{n=1}^{\infty} W_{(n)}^{*}(s)\sin(n\alpha x) \\
\overline{p}(x,s) &= \sum_{n=1}^{\infty} \overline{p}_{(n)}(s)\sin(n\alpha x)
\end{aligned}
\tag{19b}
$$

$$
\begin{aligned}
u_{\gamma}^{**0}(x,s) &= \sum_{n=1}^{\infty}\left[s^2 U_{\gamma(n)}^{*0}(s) - s\dot{U}_{\gamma(n)}^{0}(t=0) - \ddot{U}_{\gamma(n)}^{0}(t=0)\right]\cos(n\alpha x) \\
&= \sum_{n=1}^{\infty} U_{\gamma(n)}^{**0}(s)\cos(n\alpha x) \\
\phi_{\gamma}^{**}(x,s) &= \sum_{n=1}^{\infty}\left[s^2 \Phi_{\gamma(n)}^{*}(s) - s\dot{\Phi}_{\gamma(n)}(t=0) - \ddot{\Phi}_{\gamma(n)}(t=0)\right]\cos(n\alpha x) \\
&= \sum_{n=1}^{\infty} \Phi_{\gamma(n)}^{**}(s)\cos(n\alpha x) \\
w^{**}(x,s) &= \sum_{n=1}^{\infty}\left[s^2 W_{(n)}^{*}(s) - s\dot{W}_{(n)}(t=0) - \ddot{W}_{(n)}(t=0)\right]\sin(n\alpha x) \\
&= \sum_{n=1}^{\infty} W_{(n)}^{**}(s)\sin(n\alpha x)
\end{aligned}
\tag{19c}
$$

where $p_{(n)}(t)$ is the external load and $\alpha=\pi/L$. By substituting Eqs. (19b) and (19c) into the resultants given in Eqs. (14), (17a) and (17b), one can express the resultants in terms of the displacement variables. Successively, substituting the resultants obtained into the equilibrium equations given in Eq. (11), the algebraic relations between the primary variables and the external force in the Laplace domain are obtained as follows:

$$
\begin{bmatrix}
K_{11}^{*} & K_{12}^{*} & K_{13}^{*} & K_{14}^{*} & K_{15}^{*} \\
K_{21}^{*} & K_{22}^{*} & K_{23}^{*} & K_{24}^{*} & K_{25}^{*} \\
K_{31}^{*} & K_{32}^{*} & K_{33}^{*} & K_{34}^{*} & K_{35}^{*} \\
K_{41}^{*} & K_{42}^{*} & K_{43}^{*} & K_{44}^{*} & K_{45}^{*} \\
K_{51}^{*} & K_{52}^{*} & K_{53}^{*} & K_{54}^{*} & K_{55}^{*}
\end{bmatrix}
\begin{Bmatrix} U_1^{*0} \\ U_2^{*0} \\ \Phi_1^{*} \\ \Phi_2^{*} \\ W^{*} \end{Bmatrix}
+
\begin{bmatrix}
M_{11}^{*} & M_{12}^{*} & M_{13}^{*} & M_{14}^{*} & M_{15}^{*} \\
M_{21}^{*} & M_{22}^{*} & M_{23}^{*} & M_{24}^{*} & M_{25}^{*} \\
M_{31}^{*} & M_{32}^{*} & M_{33}^{*} & M_{34}^{*} & M_{35}^{*} \\
M_{41}^{*} & M_{42}^{*} & M_{43}^{*} & M_{44}^{*} & M_{45}^{*} \\
M_{51}^{*} & M_{52}^{*} & M_{53}^{*} & M_{54}^{*} & M_{55}^{*}
\end{bmatrix}
\begin{Bmatrix} U_1^{**0} \\ U_2^{**0} \\ \Phi_1^{**} \\ \Phi_2^{**} \\ W^{**} \end{Bmatrix}
=
\begin{Bmatrix} 0 \\ 0 \\ 0 \\ 0 \\ \overline{p} \end{Bmatrix}
\tag{20}
$$

where $K^*(s)$ is the global stiffness matrix, and $M^*(s)$ is global mass matrix in Laplace domain with the detail expressions which are shown in the Appendix 2 and 3. It is well recognized that all of the primary variables and the applied force depends on the Laplace variable s in Laplace domain. Differing from the elastic analysis, the basic viscoelastic effects consist of creep and relaxation. The creep process consists of the time-dependent strain resulting from the induced steady stress. The function of applied force is already given in Eq. (19a). Therefore, by solving the Eq. (20), the primary variables can be obtained. In contrast, the relaxation process consists of time-dependent stress resulting from the induced steady strain. Therefore, in the plate bending problem, the applied deflection is given as a constant.

The solutions of Eqs. (20) in Laplace domain need to be inversed to the real time domain. However, it is not possible to invert the above equations directly. We employ a numerical inverse Laplace transform technique. There are a number of numerical Laplace transform and numerical Laplace inversion transform techniques developed by Stehfest, Zakian, Cost and Becker, Schapery, Durbin or Fourier series method [29-33]. Narayanan and Beskos [32], Hassan Hassanzadeh and Mehran Pooladi-Darvish [29] have listed and compared the numerical algorithms with each other for Laplace transform inversions. In general, Fourier series method provide accurate results for both non-oscillatory and oscillatory functions. Thus, in this study, the Fourier series algorithm is employed to obtain the numerical results.

To verify the present analysis with the other theories reported previously, the [0/90/0], [0/90/0/90] and $[0/90/0/90/0]_s$ laminated composite plates are chosen as illustrative numerical examples for static bending analysis by setting the time derivative terms to be zero. The material properties as well as time-dependent relaxation modulus of graphite/epoxy GY70/399 at the room temperature (T=75°F) and low moisture (M=0.1%) are employed:

$$\begin{aligned} &E_{11} = 2.89\times10^5 MPa && E_{22} = 6.063\times10^3 MPa \\ &G_{12} = G_{13} = 4.134\times10^3 MPa && G_{23} = 2.067\times10^3 MPa \\ &\nu_{12} = 0.31 \end{aligned} \tag{21a}$$

And the other properties of laminated plate are assumed as follows:

$$\begin{aligned} &S = 4 \\ &\rho = 1480\ \ kg/m^3 \end{aligned} \tag{21b}$$

where S is length-to-height ratio, ρ is a mass density. The time-dependent function $\varphi(t)$ for GY70/399 is shown in Table.1 by mastering curve Crossman's experimental data [19].

The function of applied force is assumed as $p(t)$=1.0 for creep process, and the static applied deflection is consider as $w(t)$=1.0 for relaxation process. The displacement and stress are normalized by the following nondimensional values:

$$U_1 = \frac{100\,E_T u_1}{p_0 h S^3} \qquad W = \frac{100\,E_T w}{p_0 h S^4} \tag{22}$$

where S represents the length to thickness ratio, which is defined by $S=L/h$.

The Fig. 2 shows the time-dependent nondimensional deflection W of the symmetric laminate [0/90/0] (I), antisymmetric [0/90/0/90] (II) and symmetric with many layers $[0/90/0/90/0]_s$ (III) for creep process. At the initial time, both elastic and viscoelastic solution have the same value (We_I=1.7214, We_{II}=2.4728 and We_{III}=1.8376). After that, the elastic solution keeps the deflection value as a constant because of time-independent characteristics. The viscoelastic solutions of three cases have a good agreement for the deflection behavior. The values of nondimensional deflections begin at We and increase as time goes.

p	b_p	τ_p
0	0.669825e-1	∞
1	0.813977e-2	5.516602214e+02
2	0.484272e-1	1.494783951e+04
3	0.710360e-1	5.288067476e+05
4	0.114155e+0	1.846670914e+07
5	0.102892e+0	5.253922053e+08
6	0.146757e+0	1.799163029e+10
7	0.148508e+0	4.761315266e+11
8	0.150514e+0	1.477467149e+13
9	0.696426e-1	4.976486103e+14
10	0.729459e-1	8.174141919e+15

Table 1: The time-dependent function of relaxation modulus of GY 70/339 composite material.

Time	[0/90/0]	[0/90/0/90]	[0/90/0/90/0]s
t=0 (Elastic case)	1.7214	2.4728	1.8376
$t=10^1$s	1.7215	2.4730	1.8378
$t=10^2$s	1.7230	2.4752	1.8394
$t=10^3$s	1.7318	2.4878	1.8493
$t=10^4$s	1.7604	2.5292	1.8816
$t=10^5$s	1.8085	2.5991	1.9363
$t=10^6$s	1.8850	2.7108	2.0241
$t=10^7$s	1.9707	2.8374	2.1240
$t=10^8$s	2.1228	3.0655	2.3052
$t=10^9$s	2.2932	3.3256	2.5136
$t=10^{10}$s	2.4794	3.6173	2.7500

Table 2: The value of time-dependent nondimensional deflection W

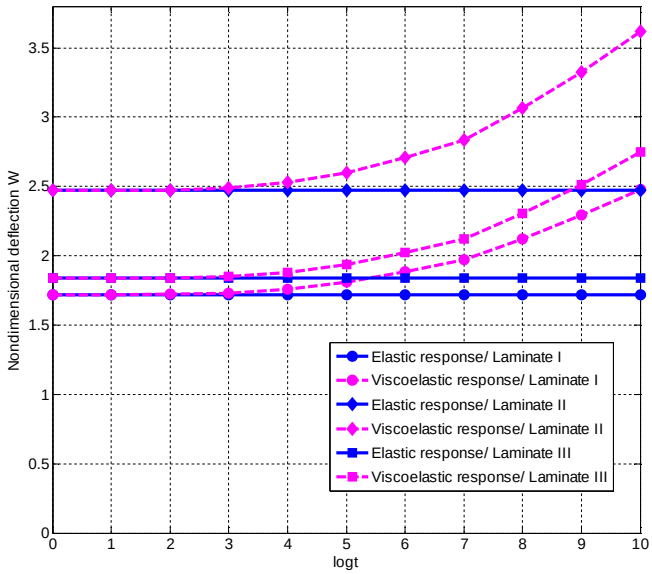

Fig. 2 The time-dependent nondimensional deflection *W*.

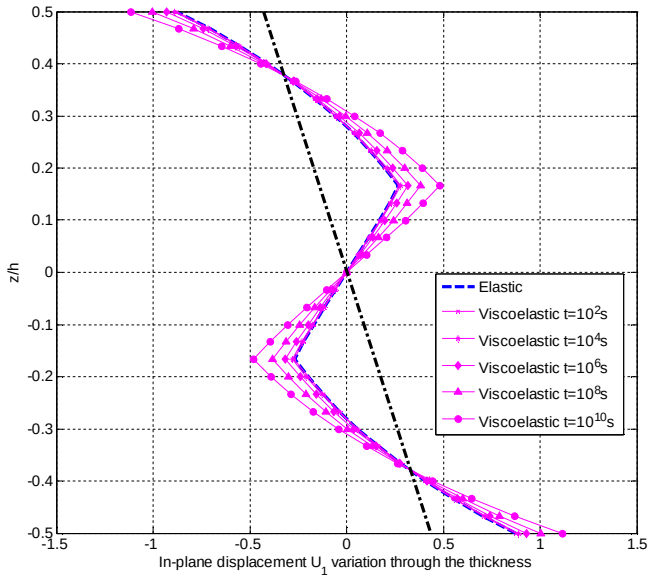

Fig. 3a The time-dependent nondimensional in-plane displacement U_1 of laminate I.

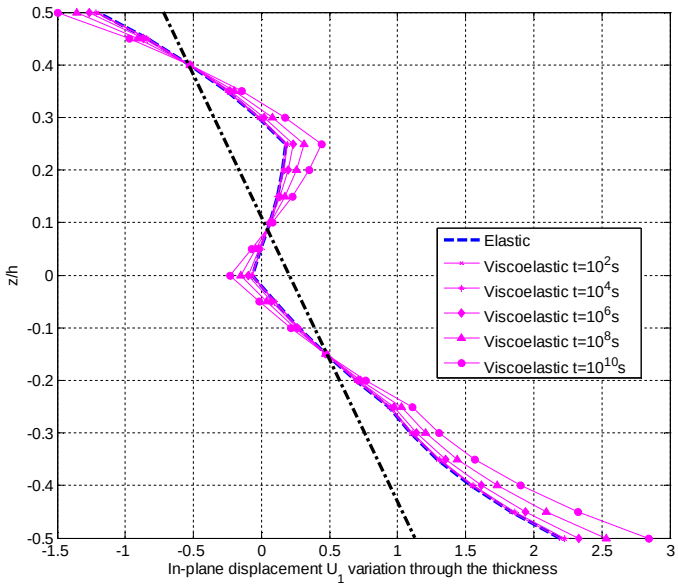

Fig. 3b The time-dependent nondimensional in-plane displacement U_1 of laminate II.

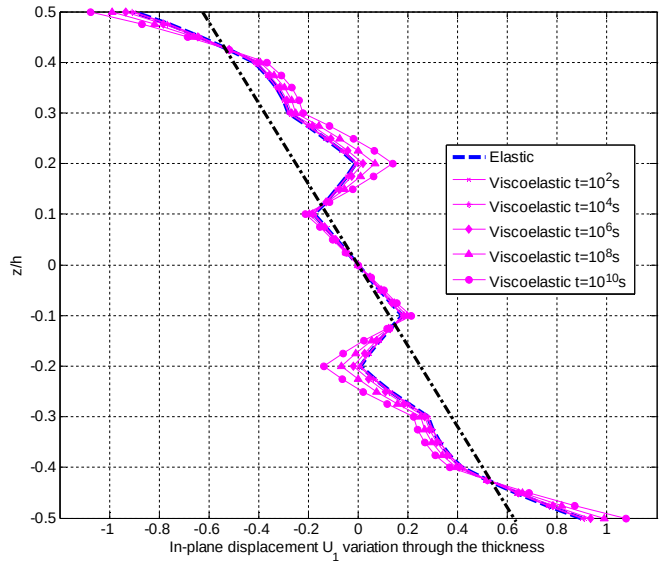

Fig. 3c The time-dependent nondimensional in-plane displacement U_1 of laminate III.

The distributions through the thickness of in-plane displacement variation U_1 are shown in Fig. 3a (I), Fig. 3b (II) and Fig. 3c (III). The in-plane displacement shows an accurate prediction for the elastic analysis [2]. For the viscoelastic analysis based on the EHOPT have a good agreement with the elastic one. The viscoelastic response has the same solution with the elastic one at the initial time. After that, it changes with respect to time but still keep the zigzag pattern through the thickness of laminates. From the distribution shown in the figure, there are some points at which the value of U_1 is constant or time-independent. For the symmetric laminate (I, III) cases, the midpoint is always the one of time-independent points. These time-independent points are belong to a straight line which shown as dot-dashed line in the figures. The difference $\Delta(t) = \left|U_1(z,t) - D(z,t)\right|$ between the in-plane displacement and the time-independent line increase with respect to the time.

The Fig. 4a, 4b and 4c show the in-plane normal stress variation through the thickness of laminate I, II and III respectively for relaxation process. The elastic responses of EHOPT show good agreements with the exact solution [2]. From the figure, we can see that: (1) at some layers whose value of normal stress is 0 at the initial time, the stress keeps the value as 0 as time proceeds. (2) We can observe a slight variation of in-plane normal stress which is dominated by the fiber direction. For instance, like the elastic solution, the viscoelastic behavior

of the normal stress σ_{11} for symmetric I and III still keep the symmetric properties.

The transverse shear stress variations through the thickness are shown in Fig. 5a, Fig. 5b and Fig. 5c for the relaxation process. The elastic solutions of EHOPT have good agreements with those of exact elasticity [2]. From the Fig. 5, we can see that: (1) at the initial time, the viscoelastic solution have same value with that of elastic problem; (2) then, the amplitude of transverse stress decreases with respect to time, but still keeps the through-the-thickness shape. Especially for the symmetric laminates, the symmetric distribution properties of transverse shear stress are conserved.

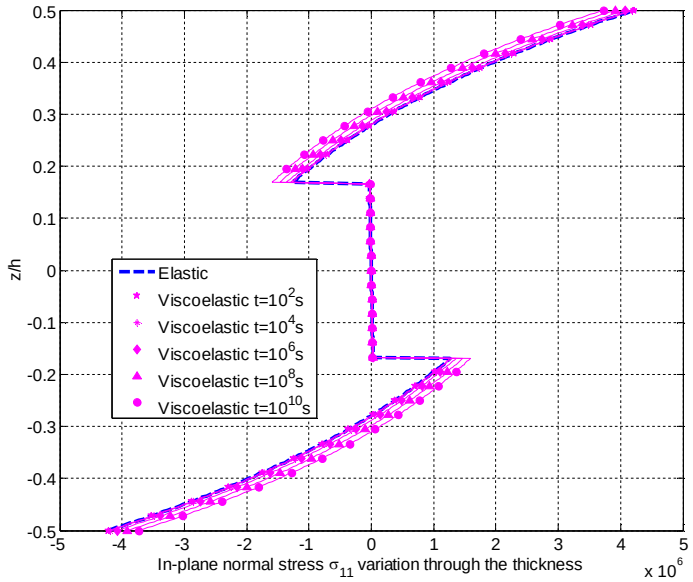

Fig. 4a The in-plane normal tress σ_{11} variation through the thickness of laminate I.

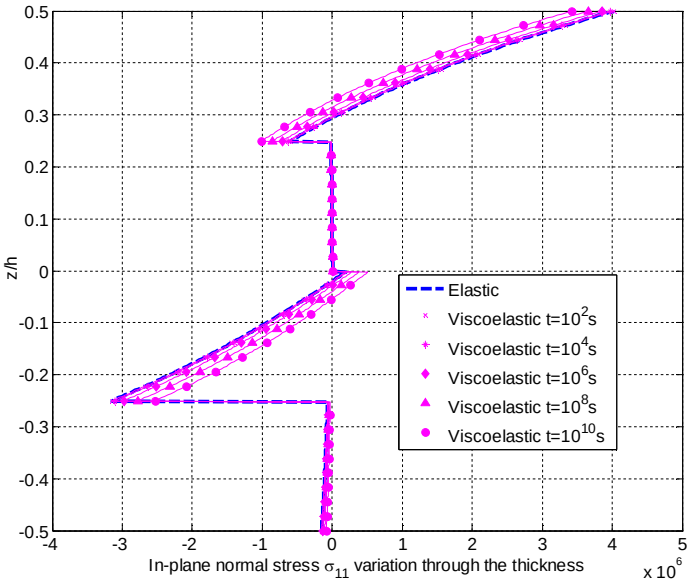

Fig. 4b The in-plane normal tress σ_{11} variation through the thickness of laminate II.

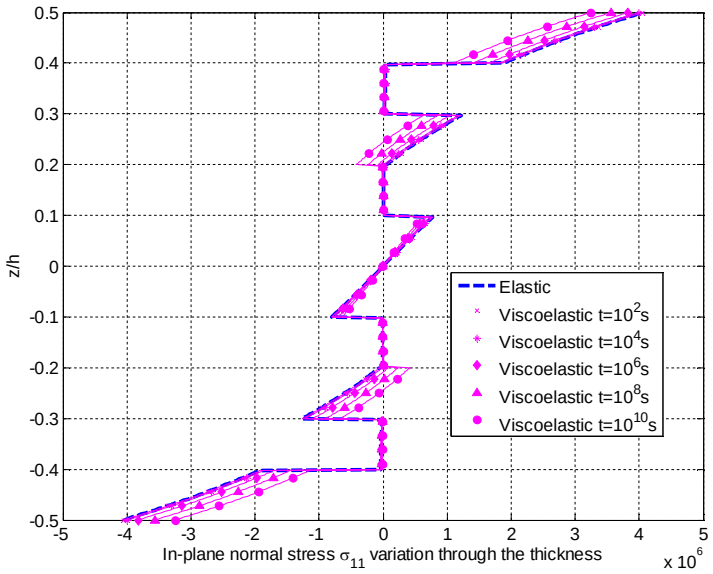

Fig. 4c The in-plane normal tress σ_{11} variation through the thickness of laminate III.

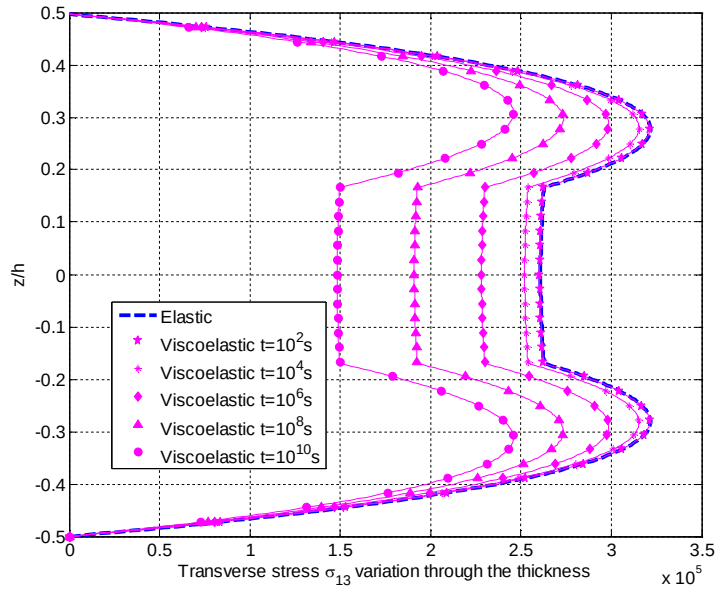

Fig. 5a The transverse stress σ_{13} variation through the thickness of laminate I.

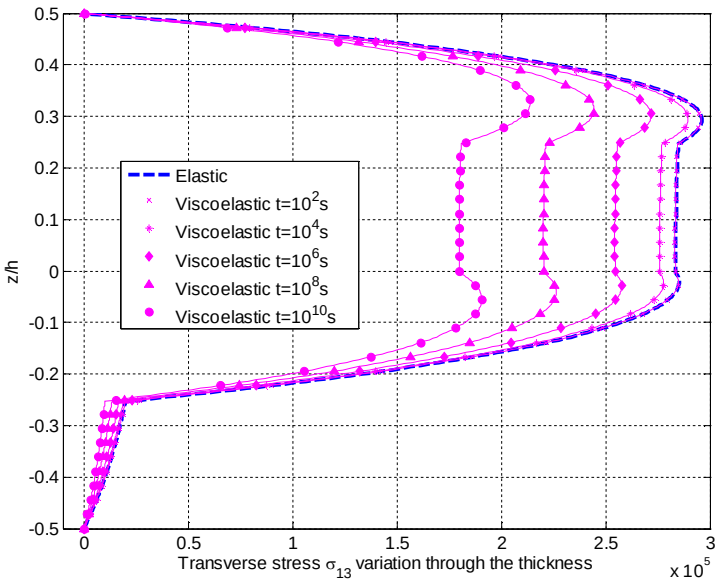

Fig. 5b The transverse stress σ_{13} variation through the thickness of laminate II.

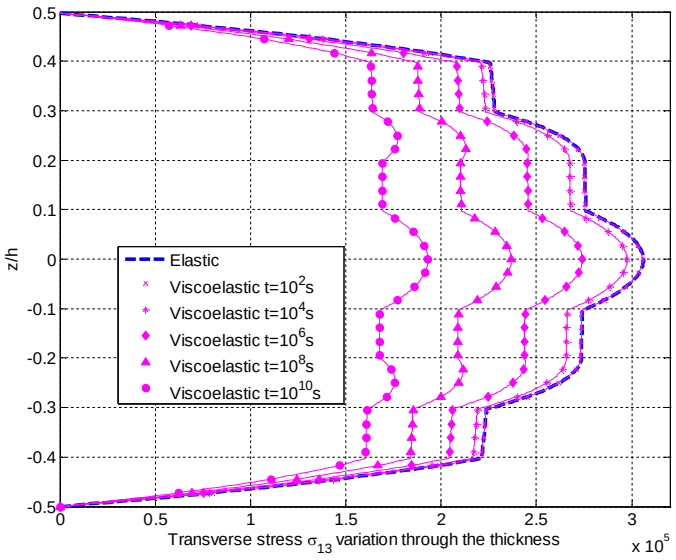

Fig. 5c The transverse stress σ_{13} variation through the thickness of laminate III.

Chapter 6. Conclusion

The mechanical behaviors of linear viscoelastic laminates based on EHOPT have been efficiently analyzed by employing the Laplace transform without any integral transformation or any time step scheme. The computational accuracy and efficiency of the analysis are retained since the viscoelastic EHOPT formulation was made in the elastic equivalence in the Laplace transformed domain. The numerical results for graphite/epoxy GY70/339 composite material adequately show the change of time-dependent mechanical behaviors such as the deflection, the in-plane displacement for creep process as well as the normal and transverse shear stress for relaxation process. The transverse stress continuity condition at the interfaces between layers can be successfully satisfied to reduce the number of unknown variables. It promises for applying viscoelastic behavior of composite laminates to various higher order models including [7, 11-12, 14, 16, 20]. Since the present analysis extended the applications of the higher order plate theories to the viscoelastic materials, it is certain that the present viscoelastic approach can provide the theoretical basis with high accuracy and efficiency for the various mechanical behavior of laminated composites.

Appendix 1: Calculation of Terms in Equation (9)

The transverse stress continuity conditions are:

$$\tau_{3\alpha}\Big|_{z=z_m^-} = \tau_{3\alpha}\Big|_{z=z_m^+} \tag{23}$$

where $m = 1, 2, ..., n-1$

The transverse stress continuity conditions at the interfaces of viscoelastic composite laminates can be expressed by the following matrix equation in the Laplace transformed domain:

$$\begin{pmatrix} Q_{3\alpha 3\gamma}^{2*} & 0 & 0 & . & 0 \\ \Delta Q_{3\alpha 3\gamma}^{2*} & Q_{3\alpha 3\gamma}^{3*} & 0 & . & 0 \\ \Delta Q_{3\alpha 3\gamma}^{3*} & \Delta Q_{3\alpha 3\gamma}^{3*} & Q_{3\alpha 3\gamma}^{4*} & . & . \\ . & . & . & . & 0 \\ \Delta Q_{3\alpha 3\gamma}^{(n-1)*} & \Delta Q_{3\alpha 3\gamma}^{(n-1)*} & . & . & Q_{3\alpha 3\gamma}^{n*} \end{pmatrix} \begin{pmatrix} S_\gamma^{1*} \\ S_\gamma^{2*} \\ . \\ . \\ S_\gamma^{(n-1)*} \end{pmatrix} = \begin{pmatrix} -\Delta Q_{3\alpha 3\gamma}^{1*} \\ -\Delta Q_{3\alpha 3\gamma}^{2*} \\ . \\ . \\ -\Delta Q_{3\alpha 3\gamma}^{(n-1)*} \end{pmatrix} \left[\chi_\gamma^* + w_{,\gamma}^* \right] + \begin{pmatrix} -2\Delta Q_{3\alpha 3\gamma}^{1*} z_1 \\ -2\Delta Q_{3\alpha 3\gamma}^{2*} z_2 \\ . \\ . \\ -2\Delta Q_{3\alpha 3\gamma}^{(n-1)*} z_{n-1} \end{pmatrix} \xi_\gamma^* + \begin{pmatrix} -3\Delta Q_{3\alpha 3\gamma}^{1*} z_1^2 \\ -3\Delta Q_{3\alpha 3\gamma}^{2*} z_2^2 \\ . \\ . \\ -3\Delta Q_{3\alpha 3\gamma}^{(n-1)*} z_{n-1}^2 \end{pmatrix} \phi_\gamma^* \tag{24}$$

where

$$\Delta Q_{3\alpha 3\gamma}^{m*}(s) = Q_{3\alpha 3\gamma}^{(m+1)*}(s) - Q_{3\alpha 3\gamma}^{m*}(s)$$

Eq. (24) can be written as following symbolic form:

$$\left[A_{3\alpha 3\gamma}^* \right]_{(n-1)\times(n-1)} \left\{ S_\gamma^* \right\}_{(n-1)\times 1} = \left\{ B_{3\alpha 3\gamma}^* \right\}_{(n-1)\times 1} \left(\chi_\gamma^* + w_{,\gamma}^* \right) + \left\{ C_{3\alpha 3\gamma}^* \right\}_{(n-1)\times 1} \xi_\gamma^* + \left\{ D_{3\alpha 3\gamma}^* \right\}_{(n-1)\times 1} \phi_\gamma^* \tag{25}$$

Substituting Eq. (7) derived from traction free boundary conditions for top and bottom surfaces into Eq. (25):

$$\left[A^*_{3\alpha 3\gamma}\right]\left\{S^*_\gamma\right\} = -\left\{B^*_{3\alpha 3\gamma}\right\}\left(\frac{3h^2}{4}\phi^*_\gamma + \frac{1}{2}\sum_{k=1}^{n-1} S^{k*}_\gamma\right) - \frac{1}{2h}\left\{C^*_{3\alpha 3\gamma}\right\}\sum_{k=1}^{n-1} S^{k*}_\gamma + \left\{D^*_{3\alpha 3\gamma}\right\}\phi^*_\gamma \tag{26}$$

$$\left[A^*_{3\alpha 3\gamma}\right]\left\{S^*_\gamma\right\} + \left\{\frac{1}{2}B^*_{3\alpha 3\gamma} + \frac{1}{2h}C^*_{3\alpha 3\gamma}\right\}\sum_{k=1}^{n-1} S^{k*}_\gamma = \left\{-\frac{3h^2}{4}B^*_{3\alpha 3\gamma} + D^*_{3\alpha 3\gamma}\right\}\phi^*_\gamma \tag{27}$$

$$\left[\bar{A}^*_{3\alpha 3\gamma}\right]\left\{S^*_\gamma\right\} = \left[\bar{B}^*_{3\alpha 3\gamma}\right]\phi^*_\gamma \tag{28}$$

$$\left\{S^{k*}_\gamma\right\} = \left[\bar{A}^*_{3\alpha 3\gamma}\right]^{-1}\left[\bar{B}^*_{3\alpha 3\gamma}\right]\phi^*_\gamma \tag{29}$$

From the above equation, unknown shear angle changes S_α^k can be expressed simply,

$$S^{k*}_\alpha = b^k_{\alpha\gamma}\phi^*_\gamma \tag{30}$$

By substituting Eq. (30) into the second equation in Eq. (7), one can express the displacement variable χ_α in terms of ϕ_α and w:

$$\chi^*_\alpha = -\left(\frac{3h^2}{4}\phi^*_\alpha + w^*_{,\alpha} + \frac{1}{2}\sum_{k=1}^{n-1} S^{k*}_\alpha\right) \tag{31}$$

$$\begin{cases} \chi^*_1 = -\left(\dfrac{3h^2}{4}\phi^*_1 + w^*_{,1} + \dfrac{1}{2}\displaystyle\sum_{k=1}^{n-1} S^{k*}_1\right) \\ \chi^*_2 = -\left(\dfrac{3h^2}{4}\phi^*_2 + w^*_{,2} + \dfrac{1}{2}\displaystyle\sum_{k=1}^{n-1} S^{k*}_2\right) \end{cases} \tag{32}$$

$$\begin{cases} \chi^*_1 = -\left(\dfrac{3h^2}{4}\phi^*_1 + w^*_{,1} + \dfrac{1}{2}\displaystyle\sum_{k=1}^{n-1}\left(b^k_{11}\phi^*_1 + b^k_{12}\phi^*_2\right)\right) \\ \chi^*_2 = -\left(\dfrac{3h^2}{4}\phi^*_2 + w^*_{,2} + \dfrac{1}{2}\displaystyle\sum_{k=1}^{n-1}\left(b^k_{21}\phi^*_1 + b^k_{22}\phi^*_2\right)\right) \end{cases} \tag{33}$$

$$\begin{cases} \chi_1^* = -\left(\dfrac{3h^2}{4} + \dfrac{1}{2}\sum_{k=1}^{n-1} b_{11}^k\right)\phi_1^* - \dfrac{1}{2}\sum_{k=1}^{n-1} b_{12}^k \phi_2^* - w_{,1}^* \\ \chi_2^* = -\dfrac{1}{2}\sum_{k=1}^{n-1} b_{21}^k \phi_1^* - \left(\dfrac{1}{2}\sum_{k=1}^{n-1} b_{22}^k + \dfrac{3h^2}{4}\right)\phi_2^* - w_{,2}^* \end{cases} \tag{34}$$

Therefore

$$\chi_\alpha^* = c_{\alpha\gamma}\phi_\gamma^* - w_{,\alpha}^* \tag{35}$$

Appendix2: Components of the stiffness matrix K^*

The components of stiffness matrix K^* in Eq. (20) are obtained by substituting Eqs. (17a) and (17b) into the equilibrium equations given in Eq. (11).

$$\begin{bmatrix} K_{11}^* & K_{12}^* \\ K_{21}^* & K_{22}^* \end{bmatrix} = \begin{bmatrix} \alpha^2 A_{1111}^{0*} & \alpha^2 A_{1121}^{0*} \\ \alpha^2 A_{2111}^{0*} & \alpha^2 A_{2121}^{0*} \end{bmatrix}$$

$$\begin{bmatrix} K_{13}^* & K_{14}^* \\ K_{23}^* & K_{24}^* \end{bmatrix} = \begin{bmatrix} \alpha^2 G_{1111}^{0*} & \alpha^2 G_{1121}^{0*} \\ \alpha^2 G_{2111}^{0*} & \alpha^2 G_{2121}^{0*} \end{bmatrix}$$

$$\begin{bmatrix} K_{15}^* \\ K_{25}^* \end{bmatrix} = \begin{bmatrix} -\alpha^3 A_{1111}^{1*} \\ -\alpha^3 A_{2111}^{1*} \end{bmatrix}$$

$$\begin{bmatrix} K_{31}^* & K_{32}^* \\ K_{41}^* & K_{42}^* \end{bmatrix} = \begin{bmatrix} K_{13}^* & K_{14}^* \\ K_{23}^* & K_{24}^* \end{bmatrix}^T$$

$$\begin{bmatrix} K_{33}^* & K_{34}^* \\ K_{43}^* & K_{44}^* \end{bmatrix} = \begin{bmatrix} H_{\alpha\omega}^* \end{bmatrix} \tag{36}$$

$$\begin{bmatrix} K_{35}^* \\ K_{45}^* \end{bmatrix} = \begin{bmatrix} -\alpha^3 G_{1111}^{1*} \\ -\alpha^3 G_{1121}^{1*} \end{bmatrix}$$

$$\begin{bmatrix} K_{51}^* & K_{52}^* \end{bmatrix} = \begin{bmatrix} K_{15}^* \\ K_{25}^* \end{bmatrix}^T$$

$$\begin{bmatrix} K_{53}^* & K_{54}^* \end{bmatrix} = \begin{bmatrix} K_{35}^* \\ K_{45}^* \end{bmatrix}^T$$

$$K_{55}^* = \alpha^4 A_{1111}^{2*}$$

where

$$H^{*}_{\alpha\omega} = \alpha^{2}\left(c_{\gamma\alpha}G^{1*}_{\gamma 1\omega 1} - \frac{1}{2h}e_{\gamma\alpha}G^{2*}_{\gamma 1\omega 1} + G^{3*}_{\alpha 1\omega 1} + \sum_{k=1}^{n-1} b^{k}_{\gamma\alpha}\left(G^{1k*}_{\gamma 1\omega 1} - z_{k}G^{0k*}_{\gamma 1\omega 1}\right)\right)$$
$$+\left(c_{\gamma\alpha}G^{0*}_{\gamma 3\omega 3} - \frac{1}{h}e_{\gamma\alpha}G^{1*}_{\gamma 3\omega 3} + 3G^{2*}_{\alpha 3\omega 3} + \sum_{k=1}^{n-1} b^{k}_{\gamma\alpha}G^{0k*}_{\gamma 3\omega 3}\right) \quad (37)$$

$$G^{i*}_{\gamma 3\alpha 3} = \left\{ c_{\omega\alpha}A^{i*}_{\gamma 3\omega 3} - \frac{1}{h}e_{\omega\alpha}A^{(i+1)*}_{\gamma 3\omega 3} + 3A^{(i+2)*}_{\gamma 3\alpha 3} + \sum_{k=1}^{n-1} b^{k}_{\omega\alpha}A^{ik*}_{\gamma 3\omega 3}\right\} \quad (38)$$

$$G^{0k*}_{\gamma 3\alpha 3} = \left\{ c_{\omega\alpha}A^{0k*}_{\gamma 3\omega 3} - \frac{1}{h}e_{\omega\alpha}A^{1k*}_{\gamma 3\omega 3} + 3A^{2k*}_{\gamma 3\alpha 3} + \sum_{f=1}^{n-1} b^{f}_{\omega\alpha}A^{0(fk)*}_{\gamma 3\omega 3}\right\} \quad (39)$$

Appendix 3: Components of the mass matrix $\mathbf{M}^*$

The components of mass matrix M in Eq. (20) are obtained by substituting Eq. (14) into the equilibrium equations given in Eq. (11).

$$\begin{bmatrix} M_{11}^* & M_{12}^* \\ M_{21}^* & M_{22}^* \end{bmatrix} = \begin{bmatrix} I_0 & 0 \\ 0 & I_0 \end{bmatrix}$$

$$\begin{bmatrix} M_{13}^* & M_{14}^* \\ M_{23}^* & M_{24}^* \end{bmatrix} = \begin{bmatrix} I_3 + J_{11}^{0*} & J_{12}^{0*} \\ J_{21}^{0*} & I_3 + J_{22}^{0*} \end{bmatrix}$$

$$\begin{bmatrix} M_{15}^* \\ M_{25}^* \end{bmatrix} = \begin{bmatrix} -\alpha I_1 \\ 0 \end{bmatrix}$$

$$\begin{bmatrix} M_{31}^* & M_{32}^* \\ M_{41}^* & M_{42}^* \end{bmatrix} = \begin{bmatrix} M_{13}^* & M_{14}^* \\ M_{23}^* & M_{24}^* \end{bmatrix}^T$$

$$\begin{bmatrix} M_{33}^* & M_{34}^* \\ M_{43}^* & M_{44}^* \end{bmatrix} == \begin{bmatrix} L_{11}^* + I_6 & L_{21}^* \\ L_{12}^* & L_{22}^* + I_6 \end{bmatrix} \tag{40}$$

$$\begin{bmatrix} M_{35}^* \\ M_{45}^* \end{bmatrix} == \begin{bmatrix} -\alpha I_4 - \alpha J_{11}^{1*} \\ -\alpha J_{12}^{1*} \end{bmatrix}$$

$$\begin{bmatrix} M_{51}^* & M_{52}^* \end{bmatrix} = \begin{bmatrix} M_{15}^* \\ M_{25}^* \end{bmatrix}^T$$

$$\begin{bmatrix} M_{53}^* & M_{54}^* \end{bmatrix} = \begin{bmatrix} M_{35}^* \\ M_{45}^* \end{bmatrix}^T$$

$$M_{55}^* = I_0 - \alpha^2 I_2$$

where

$$L^{*}_{\omega\alpha} = c_{\omega\alpha} I_4 + c_{\gamma\alpha} J^{1*}_{\gamma\omega} - \frac{1}{2h} e_{\omega\alpha} I_5 - \frac{1}{2h} e_{\gamma\alpha} J^{2*}_{\gamma\omega} + J^{3*}_{\alpha\omega} + \sum_{f=1}^{n-1} b^{f}_{\omega\alpha} \left(I^{f}_{4} - z_f I^{f}_{3} \right) + \sum_{f=1}^{n-1} b^{f}_{\alpha\gamma} \left(J^{1f*}_{\gamma\omega} - z_f J^{0f*}_{\gamma\omega} \right) \tag{41}$$

$$J^{i*}_{\alpha\omega} = c_{\alpha\omega} I_{i+1} - \frac{1}{2h} e_{\alpha\omega} I_{i+2} + \sum_{k=1}^{n-1} b^{k}_{\alpha\omega} (I^{k}_{i+1} - z_k I^{k}_{i}) \tag{42}$$

$$J^{if*}_{\alpha\omega} = c_{\alpha\omega} I^{f}_{i+1} - \frac{1}{2h} e_{\alpha\omega} I^{f}_{i+2} + \sum_{k=1}^{n-1} b^{k}_{\alpha\omega} (I^{fk}_{i+1} - z_k I^{fk}_{i}) \tag{43}$$

Bibliography

[1] Pagano, N. J., “Exact Solutions for Composite Laminates in Cylindrical Bending,” Journal of Composite Materials, Vol. 3, 1969, pp. 398.

[2] Pagano, N. J., “Exact Solutions for Rectangular Bidirectional Composite and Sandwich Plates,” Journal of Composite Materials, Vol. 4, 1970, pp. 20-34.

[3] Pagano, N. J., and Hatfield, S. J., “Elastic Behavior of Multilayered Bidirectional Composites,” AIAA Journal, Vol. 10, No. 7, 1972, pp. 931-933.

[4] Reddy, J. N., Mechanics of Laminated Composite Plates and Shells, 2nd ed., CRC Press, Florida, 2004.

[5] Reddy, J. N., and Khdeir, A. A., “Buckling and Vibration of Laminated Composite Plates Using Various Plates Theories,” AIAA Journal, Vol. 27, No. 12, 1989, pp. 1808-1817.

[6] Khdeir, A. A., Reddy, J. N., and Librescu, L., “Levy Type Solution for Symmetrically Laminated Rectangular Plates Using First-Order Shear Deformation Theory,” Journal of Applied Mechanics, Vol. 54, 1987, pp. 640-642.

[7] Reddy, J. N., “A Simple Higher-Order Theory for Laminated Composite Plates”, Journal of Applied Mechanics, Vol. 51, 1984, pp. 745-752.

[8] Cho, M., and Parmerter, R. R., “Efficient Higher Order Composite Plate Theory for General Lamination Configurations,” AIAA Journal, Vol. 31, No. 7, 1993, pp. 1299-1306.

[9] Cho, M., and Parmerter, R. R., “An Efficient higher-Order Plate Theory for Laminated Composites,” Composite Structures, Vol. 20, No. 2, 1992, pp. 113-123.

[10] Cho, M., and Parmerter, R. R., “Finite Element for Composite Plate Bending Based on Efficient higher Order Theory,” AIAA Journal, Vol. 32, No. 11, 1994, pp. 2241-2248.

[11] Cho, M., Kim, K. O., and Kim, M. H., “Efficient Higher-Order Shell Theory for Laminate Composites,” Composites Structures, Vol. 34, No. 2, 1996, pp. 197-212.

[12] Cho, M., “Postprocess Method Using Displacement Field of Higher Order Laminated Composite Plate Theory,” AIAA Journal, Vol. 34, No. 2, 1996, pp. 362-368.

[13] Cho, M., and Kim, J. S., “Four-Noded Finite Element Post-Process method Using Displacement Field of Higher Order Laminated Composite Plate Theory,” Computers & Structures, Vol. 61, No. 2, 1996, pp. 283-290.

[14] Cho, M., and Kim, J. S, “Higher-Order Zig-Zag Theory for Laminated Composites with Multiple Delaminations,” Journal of Applied Mechanics-Transactions of ASME, Vol. 68, No. 6, 2001, pp. 869-877.

[15] Kim, J. S., and Cho, M., “Buckling Analysis for Delaminated Composites Using Plate bending Elements Based on Higher-Order Zig-Zag Theory,” International Journal for Numerical Methods in Engineering, Vol. 55, No. 11, 2002, pp. 1323-1343.

[16] Cho, M., and Oh, J. H., “Higher Order Zig-zag Theory for Fully Couple Thermo-Electric-Mechanical Smart Composite Plates,” International

Journal of Solids and Structures, Vol. 41, No. 5-6, 2004, pp. 1331-1356.

[17] Oh, J. H., and Cho, M., “A Finite Element based on Cubic Zig-zag Plate Theory for The Prediction of Thermo-Elactric-Mechanical behavior,” International Journal of Solids and Structures, Vol. 41, No. 5-6, 2004, pp. 1357-1375.

[18] Li, J., and Weng, G. J., “Effect of a Viscoelastic Interphase on the Creep and Stress/Strain Behavior of Fiber-Reinforced Polymer Matrix Composites,” Composites Part B, 27B, 1996, pp. 589-598.

[19] Crossman, F. W., Mauri, R. E., and Warren, W. J., “Moisture Altered Viscoelastic Response of Graphite/ Epoxy Composite,” Advanced Composite Materials Environmental Effects, ASTM STP 658, pp. 205-220.

[20] Yi, S., and Hilton, H. H., “Hygrothermal Effects on Viscoelastic Responses of Laminated Composites,” Composites Engineering, Vol. 5, No. 2, 1995, pp. 183-193.

[21] Bradshaw, R. D., and Brinson, L. C., “Mechanical response of linear viscoelastic composite laminates incorporating non-isothermal physical aging effects,” Composite Science and Technology, Vol. 59, 1999, pp. 1411-1427.

[22] Lin, K. J., and Yi, S., “Analysis of Interlaminar Stress in Viscoelastic Composites,” International Journal of Solid Structure, Vol. 27, No. 7, 1991, pp. 929-945.

[23] Lin, K. J., and Hwang, I. H. “Thermo-Viscoelastic Analysis of Composite Materials,” Journal of Composite Materials, Vol. 23, 1989, pp. 554-569.

[24] Venkat Vallala, Annie Ruimi, and Reddy, J. N., “Nonlinear

Viscoelastic Analysis of Orthotropic Beams Using a General Third-Order Theory," Composite Structures, Vol. 94, 2012, pp. 3759-3768.

[25] Cederbaum, G., and Aboudi, J., "Dynamic Response of Viscoelastic Laminated Plates," Journal of Sound and Vibration, Vol. 133, No. 2, 1989, pp. 225-238.

[26] Chen, T. M., "The Hybrid Laplace Transform/ Finite Element Method Applied to the Quasi-Static and Dynamic Analysis of Viscoelastic Timoshenko Beams," International Journal for Numerical Methods Engineering, Vol. 38, 1995, pp. 509-522.

[27] Hilton, H. H., and Yi, S., "Anisotropic Viscoelastic Finite Element Analysis of Mechanically and Hygrothermally Loaded Composites," Composites Engineering, Vol. 3, No. 2, 1993, pp. 123-135.

[28] Chandiramani, N. K., Librescu, L. and Aboudi, J., "The Theory of Orthotropic Viscoelastic Shear Deformable Composite Flat Panels and their Dynamic Stability", International Journal Solid Structure, Vol. 25, No. 5, 1989, pp. 465-482.

[29] Hassanzadeh, H., and Pooladi-Darvish, M., "Comparison of Different Numerical Laplace Inversion Methods for Engineering Applications", Applied Mathematics and Computation, Vol. 189, 2007, pp. 1966-1981.

[30] Cost, T. L., and Becker, E. B., "A Multidata Method of Approximate Laplace Transform Inversion" International Journal for Numerical Methods in Engineering, Vol. 2, 1970, pp. 207-219.

[31] Davies, B., and Martin, B., "Numerical Inversion of the Laplace Transform: a Survey and Comparison of Methods" Journal of Computational

Physics, Vol. 33, 1979, pp. 1-32.

[32] Narayanan, G. V., and Beskos, D. E., “Numerical Operational Methods for Time-Dependent Linear Problems” International Journal for Numerical Methods in Engineering, Vol. 18, 1982, pp. 1829-1854.

[33] Dubner, H., and Abate, J., “Numerical Inversion of Laplace Transforms by Relating Them to the Finite Fourier Cosine Transform” Journal of the Association for Computing Machinery, Vol. 15, No. 1, 1968, pp. 115-123.

초 록

본 논문에서는 시간에 따른 복합재료 적층 평판의 점탄성 거동을 보다 정확하고 효율적으로 해석하기 위해서 라플라스 변환을 이용한 효율적 고차이론을 제안하였다. 적층 평판의 면내 변위장은 두께 방향으로 연속적인 3 차 다항식과 선형 지그재그 함수를 중첩한 형태로 가정하였으며, 점탄성 재료의 시간에 따른 물성치는 실험 데이터로부터 결정되는 Prony series 형태를 이용하였다.

시간 적분을 포함하는 점탄성 물질의 구성 방정식은 라플라스 변환을 이용하여 대수 방정식으로 나타낼 수 있으며, 이를 통해서 점탄성 복합재 적층 평판의 횡방향 전단 응력 연속 조건을 선형 탄성 복합재의 전단응력 연속 조건과 매우 유사한 과정으로 부과할 수 있다. 라플라스 영역에서 계산된 복합재 적층 평판의 거동은 라플라스 역변환 과정을 통해서 시간 영역에서의 거동으로 나타낸다. 따라서 보다 효율적으로 복합재 적층 평판의 점탄성 거동에 대한 해석을 수행할 수 있다.

제안된 이론의 정확성 및 효율성을 검토하기 위하여, GY70/339 의 점탄성 복합재로 구성된 적층 평판의 시간에 대한 거동 해석을 수행하였다. 수치 계산 결과의 점탄성 특성은 선형 탄성 해석 결과와의 비교를 통해서 검증하였다.